Available online at www.sciencedirect.com

SciVerse ScienceDirect

Ceramics International 39 (2013) 8453–8458

CERAMICS INTERNATIONAL

www.elsevier.com/locate/ceramint

Surface modification of $LiCoO_2$ with $Li_{3x}La_{2/3-x}TiO_3$ for all-solid-state lithium ion batteries using Li_2S–P_2S_5 glass–ceramic

Sungwoo Noh[a], Junghoon Kim[a], Minyong Eom[b], Dongwook Shin[a,b,*]

[a]Division of Materials Science & Engineering, Hanyang University, 222 Wangsimni-ro, Seongdong-gu, Seoul 133-791, Repbulic of Korea
[b]Department of Fuel Cells and Hydrogen Technology, Hanyang University, 222 Wangsimni-ro, Seongdong-gu, Seoul 133-791, Repbulic of Korea

Received 8 January 2013; received in revised form 7 April 2013; accepted 8 April 2013
Available online 15 April 2013

Abstract

To improve the electrochemical performance of all-solid-state cells using $LiCoO_2$, a nano-sized lithium lanthanum titanate ($Li_{3x}La_{2/3-x}TiO_3$; LLTO) coating is employed to modify the surface of $LiCoO_2$ via a sol–gel process. The crystalline structure of pristine $LiCoO_2$ is not affected by the coating process, and nano-sized LLTO particles uniformly adhere to the surface of the $LiCoO_2$ particle. All-solid-state cells with an In/$78Li_2S \cdot 22P_2S_5$/$LiCoO_2$ structure were constructed and tested by charge and discharge cycling at a current density of 0.06 mA cm^{-2} with a cut off voltage of 1.9–3.68 V (vs. Li–In). The all-solid-state cell using $LiCoO_2$ modified with 0.05 wt% of $Li_{0.75}La_{0.42}TiO_3$ shows the highest reversible capacity and capacity retention during all cycles. The $Li_{3x}La_{2/3-x}TiO_3$ coatings are effective in reducing the charge-transfer resistance and electrode polarization by control of the composition and coating amount of $Li_{3x}La_{2/3-x}TiO_3$ because a side reaction between the interface of $LiCoO_2$ and $78Li_2S \cdot 22P_2S_5$ glass–ceramic solid electrolyte can be suppressed.

Keywords: All-solid-state lithium ion battery; Solid electrolyte; Lithium lanthanum titanate; Surface modification

1. Introduction

Lithium ion batteries have been widely developed for portable electronic devices because they have a high energy density and a long life cycle. Recently, large-scale lithium-ion batteries for electric vehicles have attracted much attention, but deep concern over the safety of battery systems employing conventional organic liquid electrolytes hampers commercialization. The safety problems of conventional battery systems are mainly caused by intense chemical reactions with active electrode materials under elevated temperatures, leakage, and the narrow electrochemical window of liquid electrolytes [1]. Therefore, considerable efforts have been made on developing all-solid-state lithium ion batteries with improved safety.

For all-solid-state batteries, solid electrolytes with high ionic conductivity, comparable to that of liquid electrolytes, are required to achieve good electrochemical performance. Among solid electrolytes, sulfide-based electrolytes are believed to be the next generation of electrolytes for all-solid-state lithium batteries because of their high lithium ion conductivity as well as their wide electrochemical window [2–4]. However, when sulfide-based solid electrolytes and oxide cathode materials come into contact, a highly resistive layer is generated at the interface, resulting in the degradation of electrochemical performance during cycling [5,6].

To reduce the large charge-transfer resistance by suppressing the formation of the highly resistive layer, surface modification of active materials with various oxides such as $Li_4Ti_5O_{12}$, $LiNbO_3$ and Li_2O–SiO_2 has been suggested. These materials can successfully prevent direct contact but simultaneously maintain the lithium ion path between the sulfide-based solid electrolytes and oxide cathode materials [1,7,8]. However, these coating materials generally have low lithium ion conductivities, which hinder the movement of the Li ion at the interface of the sulfide-based solid electrolyte and oxide cathode materials, despite their positive functionality.

Thus, in this study, lithium lanthanum titanate ($Li_{3x}La_{2/3-x}TiO_3$; LLTO), which is known to have a high conductivity of over 10^{-4} S cm^{-1} [9,10], is firstly applied as a coating material for all-solid-state lithium batteries using sulfide electrolytes.

*Corresponding author. Tel.: +82 2 2220 0503; fax: +82 2 2220 4011.
E-mail address: dwshin@hanyang.ac.kr (D. Shin).

0272-8842/$ - see front matter © 2013 Elsevier Ltd and Techna Group S.r.l. All rights reserved.
http://dx.doi.org/10.1016/j.ceramint.2013.04.027

The composition and coating amount of LLTO are changed to enhance the electrochemical properties of all-solid-state cells employing $LiCoO_2$. In addition, the effects of the surface modification on charge–discharge behavior and charge-transfer resistance of the all-solid-state cells are discussed.

2. Experimental

The surface of $LiCoO_2$ (99.8%, Sigma-Aldrich) was modified with various compositions of lithium lanthanum titanate (LLTO), $Li_{3x}La_{2/3-x}TiO_3$ ($3x$=0.33, 0.5, and 0.75), via the citric acid-assisted sol–gel method, while the coating amounts of $Li_{3x}La_{2/3-x}TiO_3$ were also changed, maintaining the Li content at 0.75. First, LLTO sols were prepared from lithium nitrate ($LiNO_3$, 98%, JUNSEI), lanthanum (III) nitrate hydrate ($LaN_3O_9 \cdot xH_2O$, 99.9%, Sigma-Aldrich) and titanium (IV) isopropoxide ($Ti[OCH(CH_3)_2]_4$, JUNSEI) [10,11]. The sols were then diluted with distilled water and mixed with $LiCoO_2$. After stirring the sols at 80 °C for 2 h, followed by drying at 150 °C for 12 h, the $LiCoO_2$ powders, modified with various compositions and amounts of LLTO, were obtained by heat treatment of the gels at 700 °C for 4 h. The heat treatment was conducted at a lower temperature, approximately 700 °C, than the conventional sintering temperature of LLTO to inhibit the formation of secondary phases through a reaction between $LiCoO_2$ and LLTO. The crystal structure of the heat-treated LLTO at 700 °C was amorphous.

The crystal structures of $LiCoO_2$ modified with LLTO were confirmed by using an x-ray powder diffractometer (XRD; Ultima IV, Rigaku) with CuKα radiation. The morphologies and particle distributions of these samples were observed using scanning electron microscopy (FE-SEM, S-4800, HITACHI).

To fabricate all-solid-state cells, $78Li_2S \cdot 22P_2S_5$ glass–ceramic powders and indium foil (99.9975%, ALFA AESAR) were used as solid electrolytes and the anode, respectively. The $78Li_2S \cdot 22P_2S_5$ glass–ceramic was prepared using a process modified from the previously reported high energy mechanical milling process and subsequent heat-treatment [12,13]. Cathode composites were prepared by mixing the modified $LiCoO_2$, $78Li_2S \cdot 22P_2S_5$ glass–ceramic and Super P® carbon (Timcal) at a weight ratio of 39:59:2. Then, 25 mg of the cathode composite, 140 mg of the $78Li_2S \cdot 22P_2S_5$ glass–ceramic powder and indium foil (0.1 mm) were cold-pressed together under 4 metric tons in a 16Φ mold. The obtained three layered pellets were packaged in a 2032-type coin cell to perform the electrochemical measurements. All processes were performed in a dry Ar-filled glove box ($[H_2O] < 1$ ppm).

All cells were galvanostatically charged and discharged using a charge–discharge measurement device (TOSCAT-3100, Toyo System) at room temperature. The charge–discharge performance was evaluated under a constant current density of 0.06 mA cm^{-2} with cut off voltages of 1.9–3.68 V (vs. Li–In). The electrochemical impedance spectroscopy measurements of the obtained cells were performed using an impedance analyzer (Solartron 1260) in the frequency range from 0.1 Hz to 1 MHz after charging it to 3.68 V at 0.06 mA cm^{-2}.

3. Results and discussion

The XRD patterns of pristine $LiCoO_2$ (abbreviated as P-LCO) and $LiCoO_2$ modified with 0.1 wt% of $Li_{3x}La_{2/3-x}TiO_3$ ($3x$=0.33, 0.5, and 0.75) particles (abbreviated as $L_{0.33}$LTO–LCO, $L_{0.5}$LTO–LCO and $L_{0.75}$LTO–LCO, respectively) are shown in Fig. 1. The XRD patterns of all LLTO coated $LiCoO_2$, as well as pristine $LiCoO_2$, index to the stoichiometric rhombohedral structure of the $R\bar{3}m$ space group. No LLTO peaks are found because the amount of coating material is too small to be detected, and heat-treated LLTO is amorphous. Other peaks related to Li–Co–O impurity and the secondary phase, which might be formed by a reaction of $LiCoO_2$ and coating materials, are not detected after modification of the $LiCoO_2$ surface. The lattice parameters calculated from the XRD patterns using MDI JADE 5 software (Rigaku) are also shown in Table 1. The lattice parameters of pristine $LiCoO_2$ and the modified $LiCoO_2$ powders have almost the same value along the *a* and *b* axes, except for a tiny difference in the value of *c*/*a*. These results show that the surface coating does not affect the crystalline structure of the $LiCoO_2$ powders.

Fig. 2 shows the surface morphologies of pristine $LiCoO_2$ and $LiCoO_2$ modified with 0.1 wt% of $Li_{3x}La_{2/3-x}TiO_3$ ($3x$=0.33, 0.5, and 0.75). A smooth and clean surface is observed for the pristine $LiCoO_2$ particles as shown in Fig. 2 (a); while various sizes of LLTO particles are randomly distributed and adhered to the surface of the LLTO coated

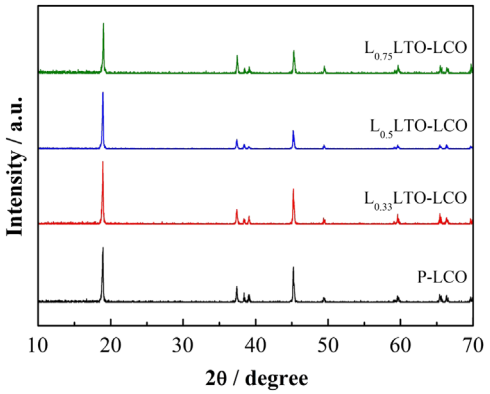

Fig. 1. XRD patterns of pristine $LiCoO_2$ (abbreviated as P-LCO), and $LiCoO_2$ modified with 0.1 wt% of $Li_{3x}La_{2/3-x}TiO_3$ ($3x$=0.33, 0.5, and 0.75) particles (abbreviated as $L_{0.33}$LTO–LCO, $L_{0.5}$LTO–LCO and $L_{0.75}$LTO–LCO, respectively).

Table 1
Lattice parameters calculated from XRD patterns of pristine $LiCoO_2$ (abbreviated as P-LCO), and $LiCoO_2$ modified with 0.1 wt% of $Li_{3x}La_{2/3-x}TiO_3$ ($3x$=0.33, 0.5, and 0.75) particles (abbreviated as $L_{0.33}$LTO–LCO, $L_{0.5}$LTO–LCO and $L_{0.75}$LTO–LCO, respectively).

Sample	$a=b$ (Å)	c (Å)	c/a
P-LCO	2.816	14.06	4.992
$L_{0.33}$LTO–LCO	2.816	14.05	4.990
$L_{0.5}$LTO–LCO	2.813	14.05	4.993
$L_{0.75}$LTO–LCO	2.816	14.06	4.992

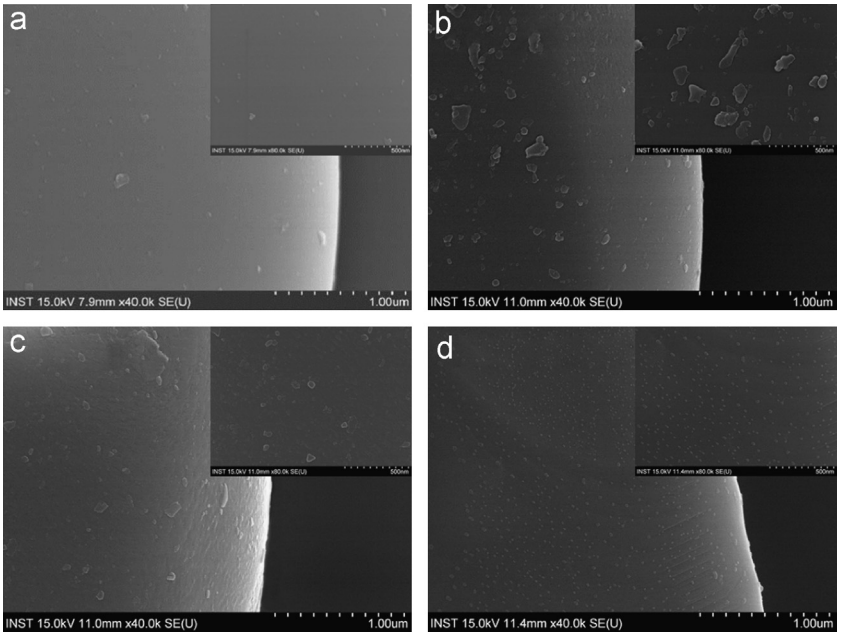

Fig. 2. SEM images of (a) pristine $LiCoO_2$ and (b)–(d) $LiCoO_2$ modified with 0.1 wt% of $Li_{3x}La_{2/3-x}TiO_3$ ($3x=0.33$, 0.5, and 0.75) particles at $\times 40{,}000$ and $\times 80{,}000$.

$LiCoO_2$. Notably, the LLTO particles show different morphologies as their composition is changed, as shown in Fig. 2(b)–(d). $L_{0.33}$LTO–LCO has a discontinuous and rough surface morphology. In contrast, the surfaces of the $L_{0.5}$LTO–LCO and $L_{0.75}$LTO–LCO powders show 60–100 and 20–30 nm LLTO particles uniformly distributed and adhered to the surface, respectively.

Fig. 3(a) shows the first charge and discharge curves of the all-solid-state cells using pristine $LiCoO_2$ and $LiCoO_2$ modified with 0.1 wt% of $Li_{3x}La_{2/3-x}TiO_3$ ($3x=0.33$, 0.5, and 0.75). The discharge capacity of the all-solid-state cell using $LiCoO_2$ modified with $L_{0.75}$LTO is the highest, approximately 127.2 mAh g^{-1} at a current density of 0.06 mA cm^{-1}, which is larger than that of cells using $LiCoO_2$ modified with $L_{0.33}$LTO or $L_{0.5}$LTO, as well as that of pristine $LiCoO_2$.

The effect of the composition of LLTO on the cycling performances (i.e., specific capacity, capacity retention as a function of the cycle number) of the all-solid-state cells are compared in Fig. 3(b). Cells using only $LiCoO_2$ modified with $L_{0.75}$LTO show a higher charge and discharge capacity during all cycles. In addition, cells using $LiCoO_2$ modified with $L_{0.75}$LTO exhibit 99.9 mAh g^{-1} of the discharge specific capacity after 30 cycles, which is higher than the corresponding value of 85.6 mAh g^{-1} for pristine $LiCoO_2$. On the other hand, all-solid-state cells using $LiCoO_2$ modified with $L_{0.5}$LTO and $L_{0.33}$LTO show lower discharge capacities of 83.69 and 66.5 mAh g^{-1}, respectively, compared to the all-solid-state cell using pristine $LiCoO_2$. Furusawa et al. reported that the lithium ion conductivity of amorphous LLTO thin films shows a monotonous increase with the increase of lithium content [14]. Although the preparation process is different between amorphous LLTO thin films and particles, it is expected that the ionic conductivity of amorphous LLTO particles adhered to the surface of $LiCoO_2$ will also increase with the increase of Li content.

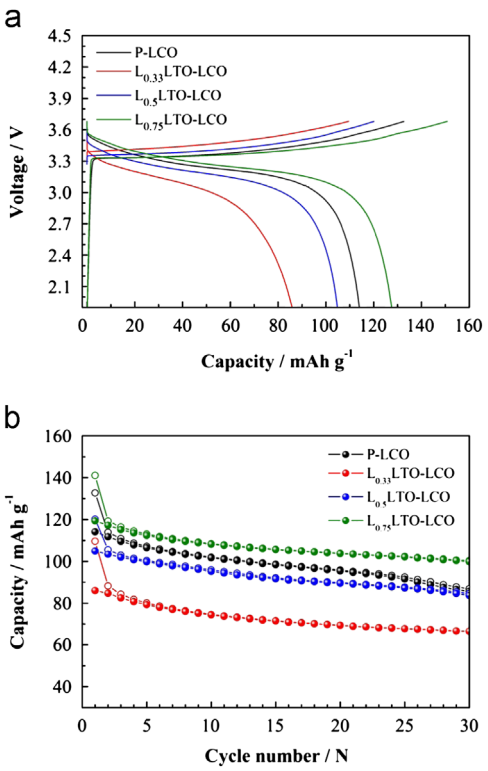

Fig. 3. (a) First charge and discharge curves and (b) specific capacity as a function of cycle number for all-solid-state cells using pristine $LiCoO_2$ and $LiCoO_2$ modified with 0.1 wt% of $Li_{3x}La_{2/3-x}TiO_3$ ($3x=0.33$, 0.5, and 0.75).

Therefore, the higher performance of all-solid-state cells using $LiCoO_2$ modified with $L_{0.75}$LTO should be related to the ionic conductivity of the coating material (LLTO).

To understand more comprehensively the effect of the composition of LLTO on cell performance, the change of charge-transfer resistance was examined by impedance spectroscopy.

Fig. 4 shows the impedance plots of all-solid-state cells using pristine $LiCoO_2$ and $LiCoO_2$ modified with 0.1 wt% of $Li_{3x}La_{2/3-x}TiO_3$ ($3x=0.33$, 0.5, and 0.75) after charging to 3.68 V (vs. Li–In) at a current density of 0.06 mA cm^{-2}.

The resistance components, which are attributed to the charge-transfer resistance at the interface between the sulfide-based solid electrolytes and the cathode active materials, are observed in the frequency region of $1–1.3\times10^3$ Hz. The calculated charge-transfer resistances of the all-solid-state cells using P-LCO, $L_{0.33}$LTO–LCO, $L_{0.5}$LTO–LCO and $L_{0.75}$LTO–LCO are 780, 1000, 935 and 640 Ω cm^2, respectively, corresponding to the variation of charge and discharge capacity with the composition of the coating material (LLTO). This result indirectly proves that LLTO possesses the optimum level of ionic conductivity to enhance the performance of all-solid-state cells, although the ionic conductivity of LLTO itself was not measured in this study. Thus, we can expect that the high reversible capacity and small charge-transfer resistance observed in the all-solid-state cell using $L_{0.75}$LTO–LCO are attributed to the suppression of the interfacial reaction by a coating of nano-sized LLTO particles. These particles must have adequate ionic conductivities that are small enough to effectively transport the lithium ions.

To achieve the optimum performance of all-solid-state cells modified with LLTO, the composition of $Li_{3x}La_{2/3-x}TiO_3$ is fixed at $Li_{0.75}La_{0.42}TiO_3$, and the amount of LLTO is varied from 0.05 to 0.2 wt%. In Fig. 5(a), the first charge and discharge curves of all-solid-state cells using pristine and $LiCoO_2$ modified with various amounts of LLTO are shown. In the initial cycle, the discharge capacities of all-solid-state cells using $LiCoO_2$ modified with 0.05 and 0.1 wt% of $L_{0.75}$LTO are higher (127.2 and 119.3 mAh g^{-1}) than that of the cell using pristine $LiCoO_2$ (114.1 mAh g^{-1}) and $LiCoO_2$ modified with 0.2 wt% of $L_{0.75}$LTO (105.5 mAh g^{-1}). In the charge and discharge capacity curves, plotted as a function of cycle number in Fig. 5(b), all the cells using $LiCoO_2$ modified with LLTO show improved cycling behavior during all cycles, except all-solid-state cells using $LiCoO_2$ modified with 0.2 wt % of $L_{0.75}$LTO.

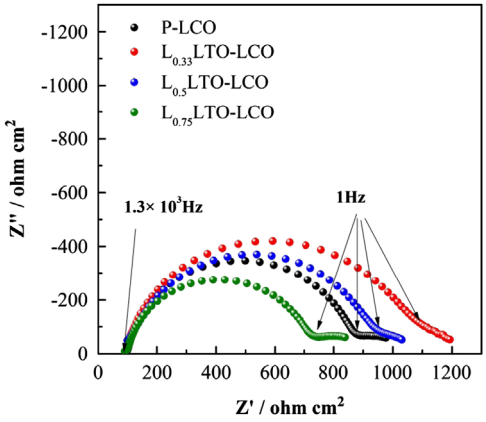

Fig. 4. Impedance plots of all-solid-state cells using pristine $LiCoO_2$ and $LiCoO_2$ modified with 0.1 wt% of $Li_{3x}La_{2/3-x}TiO_3$ ($3x=0.33$, 0.5, and 0.75) after first charging to 3.68 V.

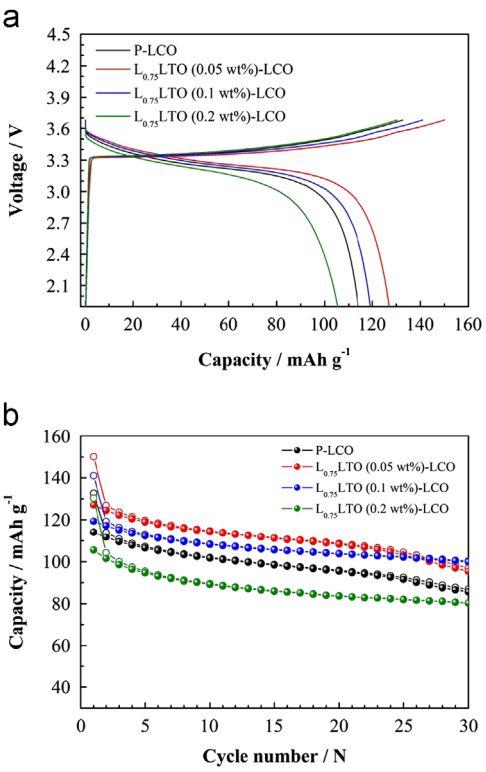

Fig. 5. (a) First charge and discharge curves and (b) specific capacity as a function of cycle number for all-solid-state cells using pristine $LiCoO_2$ and $LiCoO_2$ modified with various amounts of LLTO ($x=0.05–0.2$ wt%).

Table 2
Capacity retention values of all-solid-state cells using pristine LiCoO2 and $LiCoO_2$ modified with various amounts of $L_{0.75}$LTO after 30 cycles.

	Discharge capacity (mAh g^{-1})		Capacity retention (%) at 30 cycles
	1 cycle	30 cycles	
P-LCO	114.1	85.6	75.0
$L_{0.75}$LTO (0.05 wt%)–LCO	127.2	95.3	74.9
$L_{0.75}$LTO (0.1 wt%)–LCO	119.3	99.9	83.7
$L_{0.75}$LTO (0.2 wt%)–LCO	105.5	80.2	76.0

However, in Table 2, a more remarkable capacity fade is observed for all-solid-state cells using $LiCoO_2$ modified with 0.05 wt% of $L_{0.75}$LTO after continuous cycling despite the highest discharge capacity of 127.2 mAh g^{-1}. In contrast, the all-solid-state cell using $LiCoO_2$ modified with 0.1 wt% of $L_{0.75}$LTO shows better capacity retention of 83.7% with further cycling and the highest discharge capacity of 99.9 mAh g^{-1} after 30 cycles, despite the lower discharge capacity of the initial cycles compared with the all-solid-state cell using $LiCoO_2$ modified with 0.05 wt% of $L_{0.75}$LTO. This indicates that although the coating of nano-sized $L_{0.75}$LTO effectively enhances the cycle performance as shown in Fig. 3, excessive amounts of coating particles act as a barrier to the transport of lithium ions at the interface between the sulfide-based solid

electrolytes and oxide cathode materials, and insufficient amounts of coating particles do not completely prevent the reaction at the interface.

Fig. 6 shows the differential capacity (dQ/dV) vs. voltage profiles of the all-solid-state cells using pristine and $LiCoO_2$ modified with various amounts of LLTO at the 1st and 5th cycles. Shifts and broadening of the major redox peaks were observed in the potential range of 3.1–3.4 V with a variation of coating amounts. All cells show a similar cathodic peak potential of approximately 3.33 V in the first cycle, while a difference of cathodic peak potential between the cells using pristine and LLTO modified $LiCoO_2$ is observed after 5 cycles. Although continuous cycling causes the cathodic peaks of all the cells to shift to a higher potential, the potential shifts of all-solid-state cells using $LiCoO_2$ modified with 0.05 and 0.1 wt% of $L_{0.75}$LTO are evidently suppressed by the coating of nano-sized LLTO particles after 5 cycles. In contrast, the cathodic peak potential of the all-solid-state cell using $LiCoO_2$ modified with 0.2 wt% of $L_{0.75}$LTO shifted to a higher value than that of the all-solid-state cell using pristine $LiCoO_2$ after 5 cycles. This result shows that electrode polarization is reduced in all-solid-state cells using $LiCoO_2$ modified with 0.05 and 0.1 wt% of $L_{0.75}$LTO, which demonstrates better reversibility of the charge and discharge cycle.

In an effort to further identify the effects of the LLTO coating on the cycling performance of all-solid-state-cells, the impedance plots of fully charged all-solid-state cells, using pristine and $LiCoO_2$ modified with various amounts of LLTO in the first cycle, were analyzed (Fig. 7(a)). The calculated charge-transfer resistance of the all-solid-state cells using pristine and $LiCoO_2$ modified with 0.05, 0.1 and 0.2 wt% of $L_{0.75}$LTO are 780, 570, 640 and 900 Ω cm^2. As can be speculated from the above results, the all-solid-state cells using $LiCoO_2$ modified with 0.05 and 0.1 wt% of $L_{0.75}$LTO show smaller charge-transfer resistances, which demonstrates that their better cycling performances are closely related to the decrease in charge-transfer resistance resulting from suppression of the interfacial reaction by the coating of nano-sized LLTO particles with good ionic conductivity. In contrast, the all-solid-state cell using $LiCoO_2$ modified with 0.2 wt% of $L_{0.75}$LTO shows the largest charge-transfer resistance in spite of the good ionic conductivity of the coating material. This result indicates that excessive thickness or coverage of the coating material impedes lithium ion transportation at the interface between the solid electrolyte and active material, due to the relatively low ionic conductivity of amorphous LLTO particles relative to that of sulfide solid electrolytes and the increase of the Li ion conduction path.

The changes in charge-transfer resistance of the all-solid-state cells during 5 cycles are also shown in Fig. 7(b). After 5 cycles, the charge-transfer resistance of all the cells is gradually increased during cycling. However, the charge-transfer resistances of the all-solid-state cells using $LiCoO_2$ modified with 0.05 and 0.1 wt% of $L_{0.75}$LTO are increased to 853 and 978 Ω cm^2, respectively, which are smaller than the corresponding value of the cell using pristine $LiCoO_2$ (1209 Ω cm^2). This result shows that modification of the $LiCoO_2$ surface with nano-sized LLTO not only reduces the charge-transfer resistance in the first cycle but also suppresses the growth of charge-transfer resistance during further cycling.

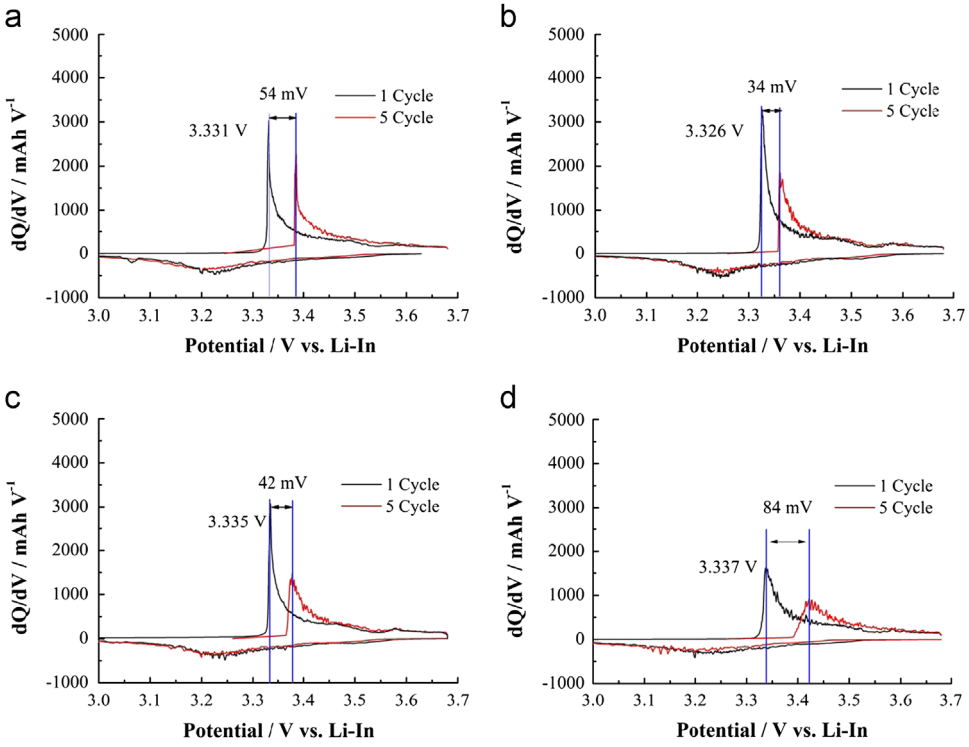

Fig. 6. Differential capacity (dQ/dV) vs. voltage profiles of all-solid-state cells using pristine and $LiCoO_2$ modified with various amounts of LLTO (x=0.05–0.2 wt %) at the 1st and 5th cycles.

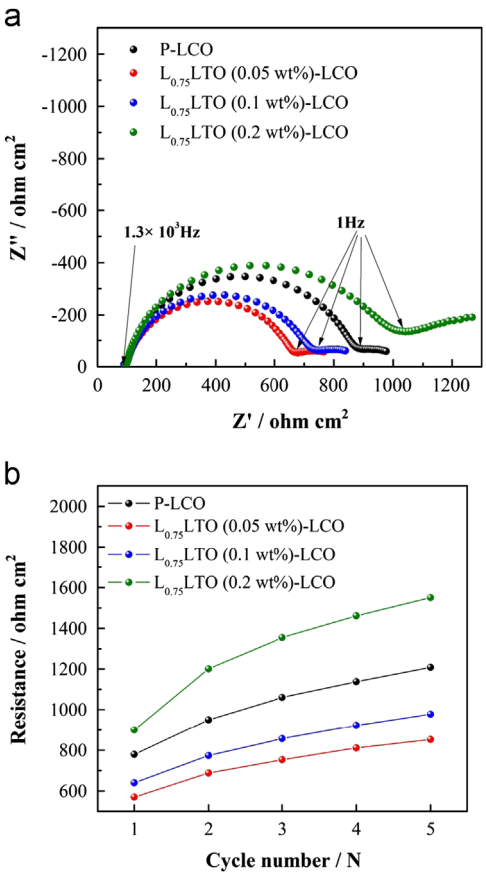

Fig. 7. (a) Impedance plots and (b) charge-transfer resistance changes of fully charged all-solid-state cells using pristine $LiCoO_2$ and $LiCoO_2$ modified with various amounts of LLTO (x=0.05–0.2 wt%).

From this work, $Li_{3x}La_{2/3-x}TiO_3$, which is known to have good ionic conductivity, was confirmed to effectively act as a coating material to suppress the interfacial reaction between sulfide-based solid electrolytes and oxide cathode materials by control of the composition and coating amount of $Li_{3x}La_{2/3-x}TiO_3$. To successfully enhance cell performance, the coating material $Li_{3x}La_{2/3-x}TiO_3$ should contain a high Li ion concentration in order to exhibit good ionic conductivity, and the coating amount covering the surface of $LiCoO_2$ should be small enough to facilitate lithium ion and electron conduction.

4. Conclusions

A $Li_{3x}La_{2/3-x}TiO_3$ coating on the surface of $LiCoO_2$ was firstly conducted via the sol–gel process to enhance the cycle performance of all-solid-state cells using sulfide electrolytes. It is identified that $Li_{3x}La_{2/3-x}TiO_3$ is an effective material to increase reversible capacity and reduce capacity fading. The coating material $Li_{3x}La_{2/3-x}TiO_3$ should contain a high lithium content to have sufficient ionic conductivity, and the amount of $Li_{3x}La_{2/3-x}TiO_3$ covering the surface of $LiCoO_2$ should not exceed 0.1 wt% of $LiCoO_2$ so that $Li_{3x}La_{2/3-x}TiO_3$ may act as an effective coating material. As a result, the all-solid-state cells using $LiCoO_2$ modified with 0.05 and 0.01 wt% of $Li_{0.75}La_{0.42}TiO_3$ showed the lower charge-transfer resistance and smaller resistance increase during all cycles through the suppression of the interfacial reaction between the sulfide solid electrolyte and oxide cathode material, leading to smaller electrode polarization and eventually better cycle performance.

Acknowledgment

This research was supported by a grant from the Fundamental R&D Program for Core Technology of Materials funded by the Korean Ministry of Knowledge Economy (Grant no. 10037233).

References

[1] H. Kitaura, A. Hayashi, K. Tadanaga, M. Tatsumisago, Improvement of electrochemical performance of all-solid-state lithium secondary batteries by surface modification of $LiMn_2O_4$ positive electrode, Solid State Ionics 192 (2011) 304–307.
[2] J. Kim, Y. Yoon, J. Lee, D. Shin, Formation of the high lithium ion conducting phase from mechanically milled amorphous Li_2S–P_2S_5 system, Journal of Power Sources 196 (2011) 6920–6923.
[3] Y. Seino, K. Takada, B.C. Kim, L. Zhang, N. Ohta, H. Wada, M. Osada, T. Sasaki, Synthesis of phosphorous sulfide solid electrolyte and all-solid-state lithium batteries with graphite electrode, Solid State Ionics 176 (2005) 2389–2393.
[4] N. Kamaya, K. Homma, Y. Yamakawa, M. Hirayama, R. Kanno, M. Yonemura, T. Kamiyama, Y. Kato, S. Hama, K. Kawamoto, A. Mitsui, A lithium superionic conductor, Nature Materials 10 (2011) 682–686.
[5] N. Ohta, K. Takada, L. Zhang, R. Ma, M. Osada, T. Sasaki, Enhancement of the high-rate capability of solid-state lithium batteries by nanoscale interfacial modification, Advanced Materials 18 (2006) 2226–2229.
[6] A. Sakuda, A. Hayashi, M. Tatsumisago, Interfacial observation between $LiCoO_2$ electrode and Li_2S–P_2S_5 solid electrolytes of all-solid-state lithium secondary batteries using transmission electron microscopy, Chemistry of Materials 22 (2010) 949–956.
[7] N. Ohta, K. Takada, I. Sakaguchi, L. Zhang, R. Ma, K. Fukuda, M. Osada, T. Sasaki, $LiNbO_3$-coated $LiCoO_2$ as cathode material for all solid-state lithium secondary batteries, Electrochemistry Communications 9 (2007) 1486–1490.
[8] A. Sakuda, H. Kitaura, A. Hayashi, K. Tadanaga, M. Tatsumisago, Modification of interface between $LiCoO_2$ electrode and Li_2S–P_2S_5 solid electrolyte using Li_2O–SiO_2 glassy layers, Journal of the Electrochemical Society 156 (2009) A27–A32.
[9] Y. Inaguma, C. Liquan, M. Itoh, T. Nakamura, T. Uchida, H. Ikuta, M. Wakihara, High ionic conductivity in lithium lanthanum titanate, Solid State Communications 86 (1993) 689–693.
[10] H. Geng, J. Lan, A. Mei, Y. Lin, C.W. Nan, Effect of sintering temperature on microstructure and transport properties of $Li_{3x}La_{2/3-x}TiO_3$ with different lithium contents, Electrochimica Acta 56 (2011) 3406–3414.
[11] B. Antoniassi, A.H.M. González, S.L. Fernandes, C.F.O. Graeff, Microstructural and electrochemical study of $La_{0.5}Li_{0.5}TiO_3$, Materials Chemistry and Physics 127 (2011) 51–55.
[12] M. Tatsumisago, F. Mizuno, A. Hayashi, All-solid-state lithium secondary batteries using sulfide-based glass–ceramic electrolytes, Journal of Power Sources 159 (2006) 193–199.
[13] J. Kim, M. Eom, S. Noh, D. Shin, Performance optimization of all-solid-state lithium ion batteries using a Li_2S–P_2S_5 solid electrolyte and $LiCoO_2$ cathode, Electronic Materials Letters 8 (2012) 209–213.
[14] S.I. Furusawa, H. Tabuchi, T. Sugiyama, S. Tao, J.T.S. Irvine, Ionic conductivity of amorphous lithium lanthanum titanate thin film, Solid State Ionics 176 (2005) 553–558.